Investigation of Boundary Layer Behaviour in HCCI Combustion using Chemiluminescence Imaging

Persson, Håkan; Hildingsson, Leif; Hultqvist, Anders; Johansson, Bengt; Ruebel, Jochen

Published in:
SAE Transactions, Journal of Fuels and Lubricants

2005

2005-01-3729

Investigation of Boundary Layer Behaviour in HCCI Combustion using Chemiluminescence Imaging

H. Persson, L. Hildingsson, A. Hultqvist and B. Johansson
Lund Institute of Technology

J. Ruebel
University of Karlsruhe

ABSTRACT

A five-cylinder diesel engine, converted to a single cylinder operated optical engine is run in Homogeneous Charge Compression Ignition (HCCI) mode. A blend of iso-octane and n-heptane is used as fuel.

An experimental study of the horizontal boundary layer between the main combustion and the non-reacting surface of the combustion chamber is conducted as a function of speed, load, swirl and injection strategy. The combustion behaviour is monitored by chemiluminescence measurements.

For all cases an interval from -10 to 16 crank angles after top dead center (CAD ATDC) in steps of one CAD are studied. One image-intensified camera observes the boundary layer up close from the side through a quartz cylinder liner while a second camera has a more global view from below to see more large scale structure of the combustion.

The averaged chemiluminescence intensity from the HCCI combustion is seen to scale well with the rate of heat release. A boundary layer is defined and studied in detail between the main combustion volume and the piston crown surface as a function of crank angle. The boundary layer is found to be in the range from 2 to 4 mm for all cases by the definition used; however, the location for the measurements becomes more and more important as combustion becomes more inhomogeneous. To get accurate calculations, the level of noise must also be considered and definitions of boundary layer thickness should not be made at to low chemiluminescence intensity.

INTRODUCTION

Homogenous Charge Compression Ignition (HCCI) is known as a combustion concept that combines some of the features of both the spark ignition (SI) and the compression ignition (CI) engine. As the SI engine, it runs with a premixed charge of fuel and oxidizer, and as the CI engine, it runs un-throttled. The main benefits of HCCI combustion are: high efficiency similar to the diesel engine, low emissions of NO_x due to low combustion temperature and also, no smoke. The challenge for HCCI combustion compared to SI and CI engines is that ignition timing depends on the in-cylinder temperature and is not directly controlled.

The early studies of HCCI combustion were made on two-stroke engines in an effort to reduce the hydrocarbon (HC) emissions at part load operation [1]. Later, in 1983, Najt and Foster showed that it was possible to attain HCCI combustion in 4-stroke engines [2]. Studies have reported low NOx emissions and high efficiency compared to the SI-engine [3]. More recent studies have been performed on both combustion stability and control [4-7]. In HCCI combustion, the premixed charge is compressed until the point of auto ignition. The more or less homogeneous charge starts to react almost simultaneously throughout the combustion chamber. However, some in-homogeneity in the combustion can be observed, and also a boundary layer exists between the strongly reacting charge in the main part of the combustion chamber compared to close to the cylinder head and piston crown where little or no reaction takes place.

One way to characterize the combustion behaviour closer is to make chemiluminescence measurements. Earlier experiments and simulations have been conducted in this area for HCCI combustion [8-10].

The intention of this study is to thoroughly investigate the combustion boundary layer. The boundary layer is defined as the area enclosed between the high reacting zone and the low reacting outer part near the combustion chamber surface. It is characterized by a steep decrease in local temperatures due to the comparably low wall temperature. Stratification of temperature has been indicated to be one possible way of extending the burn duration in HCCI and thus enable higher load without excessive pressure derivatives.

Changing the boundary layer thickness has direct influence on the thermal stratification inside the cylinder and is supposed to be a possible way of affecting the burn duration.

The main intention is to see how the boundary layer behaves when changing the operating conditions in terms of speed (turbulence), load (equivalence ratio), swirl (mixing), injection strategy (homogeneity). A correlation from the boundary layer behaviour to the impact of this on the combustion process as such is also done.

EXPERIMENTAL

ENGINE SETUP

The engine used is based on a five-cylinder Volvo diesel. The engine is modified for single cylinder operation, which gives a displacement of 0.5 liters with optical access. Engine specifications are given in Table 1 and the experimental setup can be seen in Figure 1.

Displacement	0.48 l
Valves per cylinder	4
Bore	81 mm
Stroke	93.15 mm
Compression ratio	12:1
Fuel	50/50 iso-octane/n-heptane

Table 1. Engine Data

The operating cylinder is equipped with a Bowditch piston extension. A quartz window, with a diameter of 58 mm in the elongated piston gives optical access to the combustion chamber from below. As the glass is flat, there is no bowl-in-piston as in the production engine, resulting in a pancake combustion chamber.

A quartz ring is mounted as an elongation of the cylinder liner for horizontal optical access to the upper part of the combustion chamber. The quartz liner has a height of 25 mm which gives full access to the disk shaped combustion chamber close to top dead center (TDC).

The in-cylinder pressure is monitored using an un-cooled AVL GU12S pressure transducer with a resolution of 0.2 crank angles (CAD). The pressure transducer is placed in the glow plug hole. Fuel is supplied either by port injection (PFI) or by direct injection (DI) by a five-hole nozzle, at 1000 bar. The fuel used for all measurements consists of 50% iso-octane and 50% n-heptane. Fuel consumption is measured by a fuel balance. An electrical intake heater is utilized to control combustion timing. The emission analysis equipment consists of a flame ionization detector (FID) for measuring HC, a chemiluminescence detector (CLD) for measuring nitrogen oxides (NO_x), a non dispersive infra red (NDIR) detector for measuring carbon dioxide (CO_2) and carbon monoxide (CO) and a paramagnetic detector for measuring oxygen (O_2). Smoke is not measured.

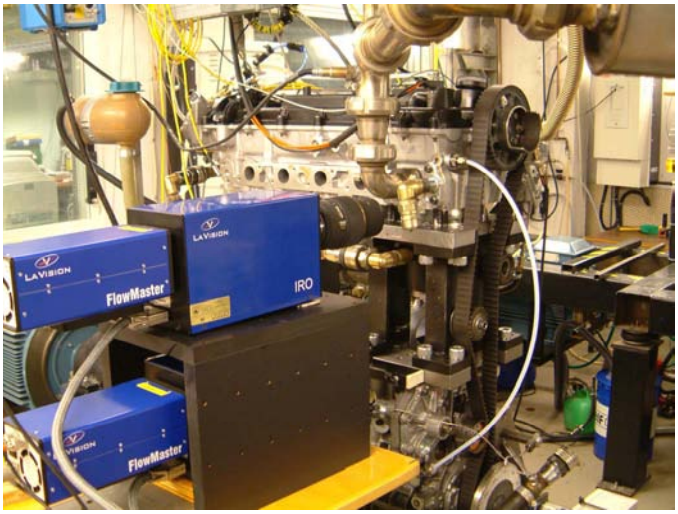

Figure 1. Experimental setup with the upper camera looking through the quartz liner and the lower camera through the piston extension from below.

CAMERA SETUP

For the chemiluminescence measurements a LA-Vision camera system was used. It consists of two CCD cameras with image intensifiers connected to a control computer. Both cameras are configured to take images simultaneously. The upper camera is mounted so it has focus in the center of the combustion chamber, giving a horizontal view through the quartz liner. The lower camera views the combustion from below through the quartz window in the piston with help of a 45° mirror placed in the piston extension.

The CCD chip resolution is 1280 x 1024 pixels. An intensifier gate time of 100 µs is used for all measurements. Both cameras are equipped with 105 mm f 2.8 macro lenses. The lens used for the boundary layer measurement is set to an aperture of f 4 and will give a depth of view of approximately 0.4 mm. When having the optics in the same height as the clearance volume, both the piston and cylinder head will block some of the light from the lens. This will create a so called optical boundary layer in the range of 8 mm vertically from both the cylinder head and piston crown. As a result, the intensity will be slightly under-estimated closer to the piston and cylinder head surfaces.

For this study only natural light is observed, no filters are used.

MEASURING PROCEDURE

For each operating point the measurement interval reaches from –10 to 16 CAD ATDC with a resolution of one CAD. For each CAD, 50 images are collected and used as well for single cycle information as for averaged. Since only one image per cycle can be acquired, all boundary layer calculations are based on the average of 50 images. The cylinder pressure is measured simultaneously making it possible to connect single cycle images to the corresponding pressure traces. All cases are run with a constant combustion timing with crank angle for 50% burned fuel mass (CA50) at approximately 3 CAD ATDC. CA50 is kept constant within +/- 0.5 CAD by moderating the intake temperature. After each measurement sweep, motored pressure traces are saved and used to verify proper operating conditions for the engine.

A base case is used as reference. This is run at 2 bar IMEPnet (entire cycle), PFI and unblocked swirl valve at 1200 rpm. Four different sweeps are made, changing one parameter at the time: load, speed, injection strategy and swirl as shown in Table 2.

sweep	swirl valve	inj. strategy	load	speed
			1.0 bar	700 RPM
			1.5 bar	900 RPM
base case	0% (open)	PFI	2.0 bar	1200 RPM
	25 %	DI -180°	2.5 bar	1500 RPM
	50 %	DI -130°	3.0 bar	
	75 %	DI -90°		
	100 % (fully blocked)	DI -50°		
		DI -30°		

Table 2. Measurement conditions.

BOUNDARY LAYER DEFINITION

The boundary layer is defined as the area enclosed between the high reacting zone and the low reacting outer part near the combustion chamber surface. The steep temperature gradient in the boundary layer is indicated by a high decrease in chemiluminescence intensity towards the combustion chamber surface. Therefore chemiluminescence imaging can be used to calculate the boundary layer behaviour. For these calculations the boundary layer is defined as the area from 15 to 85 % of maximum intensity at each crank angle. These intensities are calculated from the mean images of 50 cycles taken through the quartz liner. One such image is shown in Figure 2. By averaging these images in the horizontal direction a one-dimensional intensity is obtained. From this information the average boundary layer is obtained. For the camera system, an optical boundary effect was mentioned giving less intensity at the walls. Since the measurements are comparative, and the effect is the same in all cases, no attempts to exclude the phenomena are needed.

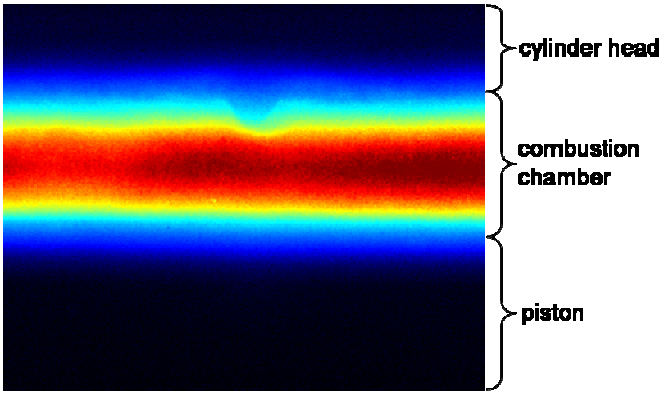

Figure 2 Averaged horizontal view of combustion through the quartz liner with injector clearly visible in the center. Image taken at point of CA50 at 3 CAD ATDC.

RESULTS

The correlation between rate of heat release and chemiluminescence intensity is of great interest for accepting the proposition that chemiluminescence intensity is a measure of global heat release in a flame. Although this proposition is commonly accepted and has been approved in previous studies [9], it is checked again with the current data to assure the measurement quality.

The maximum chemiluminescence intensity at each crank angle scales well against the rate of heat release as can be seen in Figure 3 for the reference case.

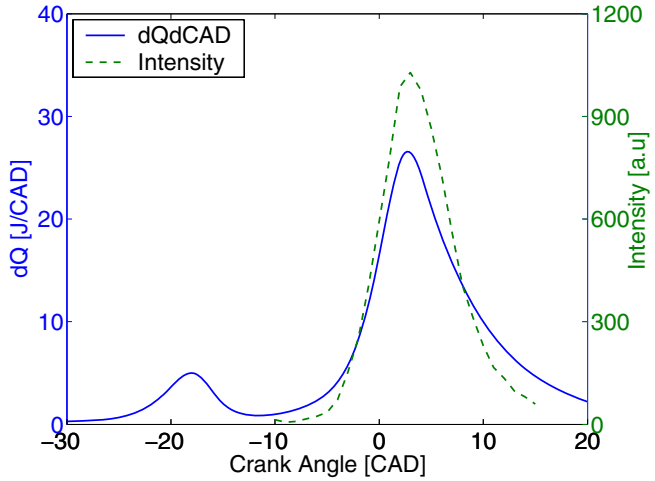

Figure 3. Rate of heat release and maximum chemiluminescence intensity for the base case.

The dotted curve in Figure 3 shows maximum intensity of natural light, starting at 10 CAD BTDC. The solid line shows the rate of heat release. As can be seen it is a two stage combustion with low temperature reactions (LTR) due to the n-heptane, followed by high temperature reactions (HTR). As the pre reactions have a low reaction rate and emit light partially in the ultra violet (UV) region, the LTR can only be faintly seen. Therefore the signal to noise ratio (SNR) in this area is too low, and because of that this region is not investigated.

For further statistical analyses of the correlation between rate of heat release and intensity, the average intensities of the measurements at each crank angle are matched with the corresponding values of the instant rate of heat release, giving the scatter plot shown in Figure 4. The intensity in this figure is calculated from the images taken from below through the piston crown.

A trend line of linear regression is also fitted to the scatter plot, showing a strong linear relationship between the rate of heat release and intensity. To quantify this relationship, the coefficient of determination R^2 is calculated. This coefficient is further explained in the appendix. For this case an R^2-value of 98.56% is calculated referring to a very strong linear relationship between the rate of heat release and average intensity. In Figure 5 this is calculated from the side images used for boundary layer calculations. Here it is seen that the horizontal averaged maximum intensity also shows very good linear correlation with R^2 of 98.69%.

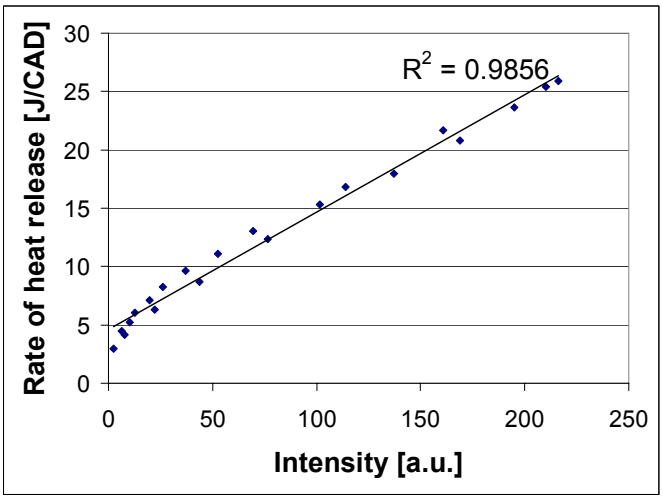

Figure 4. Variation of image average intensity versus rate of heat release and linear trend line for the base case, calculated from the intensity measured through the piston crown.

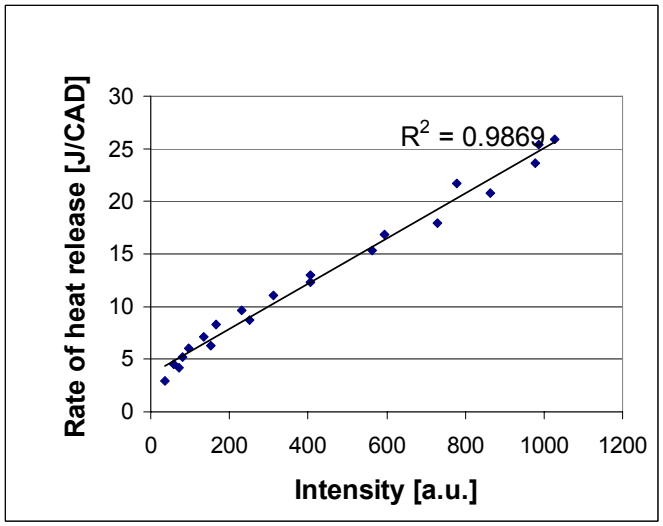

Figure 5. Variation of image average maximum intensity versus rate of heat release and linear trend line for the base case, calculated from the intensity measured horizontal through the glass liner.

Figure 3 shows the maximum chemiluminescence intensity at each CAD, this can be compared to the one-dimensional intensity distribution in Figure 6. Figure 6 shows the distribution with the cylinder head up front in the figure (~3.5mm) and the piston side in the back (~12 mm, at TDC). The plot goes from –10 to 14 CAD ATDC. As can be seen in both Figure 3 and Figure 6, the intensity does not begin to increase until just before top dead center. Because of the low signal at early CAD:s giving low SNR also for the average images, the boundary layer calculations are not very good until just before –5 CAD ATDC. The images collected for the boundary layer calculations are focused in the center of the combustion chamber from the exhaust side of the engine. The width of the images is about 28 mm and in height they stretch both slightly up over the combustion chamber and down on the piston. An image is shown in Figure 2 of this view; also the tip of the direct injector can be seen. The results shown further on are based on the boundary layer between the piston and the main combustion volume. At the upper boundary layer, the noise level was higher and therefore the lower one was chosen for evaluation.

The boundary layer calculations are as mentioned above based on horizontal averaging of the mean images. Using single points instead of average values will introduce so much noise that it is impossible to interpret data from the different cases; this is visible by the naked eye looking at Figure 2. Tests were conducted using different length and location of the averaging, all giving similar differences between the sweeps, although not exactly the same thickness. Using a longer averaging distance makes the obtained thickness more relevant for comparison between the different sweeps. Therefore the whole image width of 28 mm is chosen.

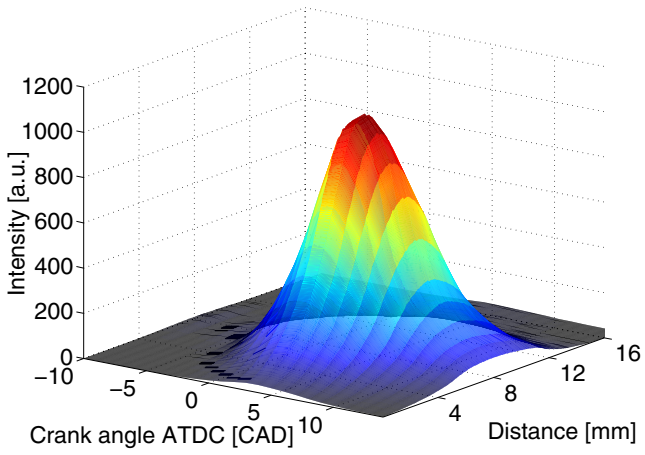

Figure 6. Averaged one-dimensional intensity from –10 to 14 CAD ATDC. Cylinder head located at approximately 3.5 mm and piston crown at 12 mm (at TDC).

Since only one image can be taken for an individual cycle it again makes sense to use an average image at each CAD for the boundary layer calculations. Yet to get some information about the changes from cycle to cycle Figure 7 shows a variation coefficient based on the standard deviation from the single images at each CAD divided by the mean intensity at each CAD for the base case. The figure shows each crank angle from the side view camera as shown for a mean intensity image in Figure 2. What is obvious is the high cycle to cycle variation at the start of main combustion, especially where the boundary layer is situated. Comparing to the rate of heat release in Figure 3, it can be seen that for increasing burn rate the variations from cycle to cycle decrease rapidly, becoming low during the main combustion. For late crank angles the cycle to cycle variations increase slightly again, now mainly at the area of the main combustion while the boundary layer shows less variations.

To get an overview of the results from the different sweeps, the duration of 10 to 90 percent burnt is showed in Figure 8. The swirl case (squares), starting to the left with fully open swirl valve, then 25% blocked, 50%, 75% and finally fully blocked, changing the swirl number from 2 to 2.6. The DI case (triangles) with injection at 180, 130, 90, 50 and 30 CAD BTDC. The load case (stars) stretches from 1 bar IMEPnet to 1.5, 2, 2,5 and 3 bar IMEP. Finally, the speed sweep (diamonds) reaches from 700rpm in the left of the figure, then 900, 1200 and 1500 rpm.

For the swirl case, no change in burn duration is observed. Pressure data only shows an average of the in-cylinder conditions so even if combustion is affected by the swirl sweep, it cannot be seen from the burn duration.

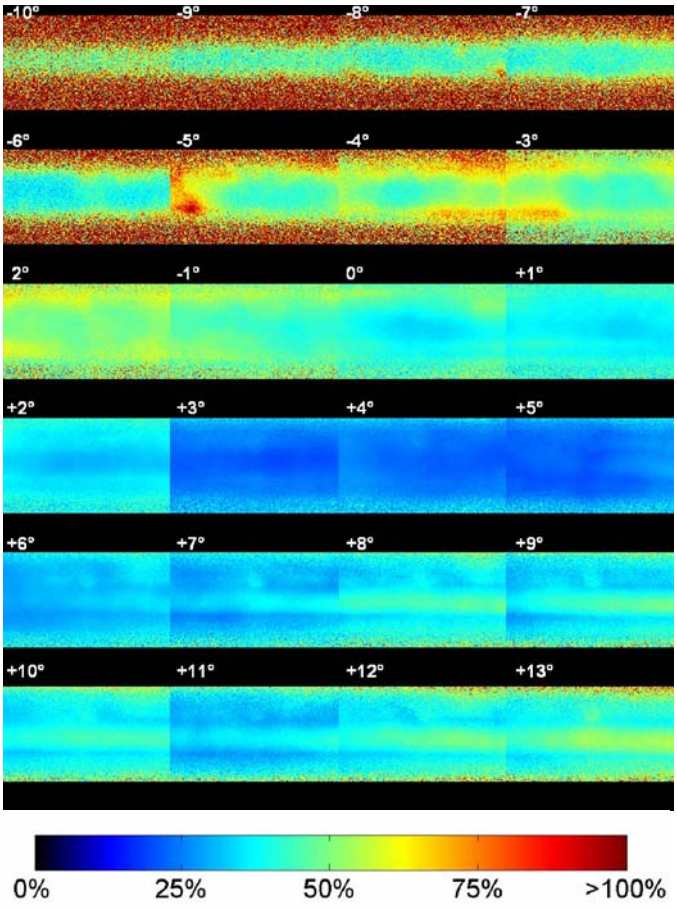

Figure 7. Variation coefficient for single images at each CAD (ATDC) for one of the base cases.

For the DI case, the burn duration is overall faster, most likely due to a more inhomogeneous charge. This is even more obvious at later injection timing when combustion duration gets shorter due to rich zones burning faster. At this point NOx is starting to form from parts of a ppm for early injection timing to a level close to 10 ppm for late injection.

In the load sweep the load was changed by altering the amount of fuel injected into the inlet port. Thereby the air/fuel ratio varied from 6.5 for low load to 4.0 for 3.0 bar IMEP. The lowest points of the load sweep have, as could be expected, the longest burn duration also compared to the other sweeps. For higher loads the richer mixture burns faster with a steeper rate of heat release and shorter burn duration.

For the speed sweep the burn duration changes dramatically when going from 1200 to 1500 rpm. At lower speed than 1200 rpm no prominent change can be seen. Increasing speed will both increase turbulence and decrease heat losses. Earlier results have shown longer combustion duration for HCCI due to increased turbulence [11]. Here the turbulence effect is lower than the effect of a hotter charge due to less heat losses.

Also the exhaust backpressure increased resulting in more trapped residuals, which also increases temperature and thus burn rate.

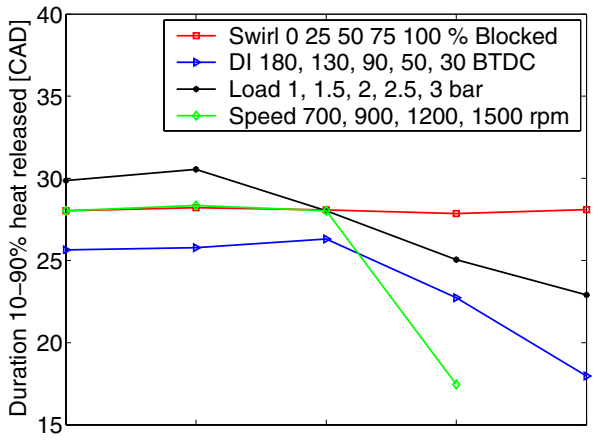

Figure 8. 10 to 90 percent burnt duration for the different sweeps. Different conditions from left to right side of the figure.

Since the engine piston has to run without oil lubrication the piston rings made out of rylon wear out quite fast. To ensure that the operating conditions are kept the same throughout the measurement campaign, new base cases have been taken during the measurements. The different base cases are shown in Figure 9. The sweeps were taken in the order that follows: First the swirl base case (diamonds), then the complete swirl sweep. Next was the DI case, for this case the injection system was modified and no base case was taken. Then the speed sweep was taken, after this a new base case was collected, the speed/load case (triangles) followed by the complete load sweep. This was followed by a final base case (squares). For all three cases the intake temperature and the corresponding motored peak pressure was in a narrow range.

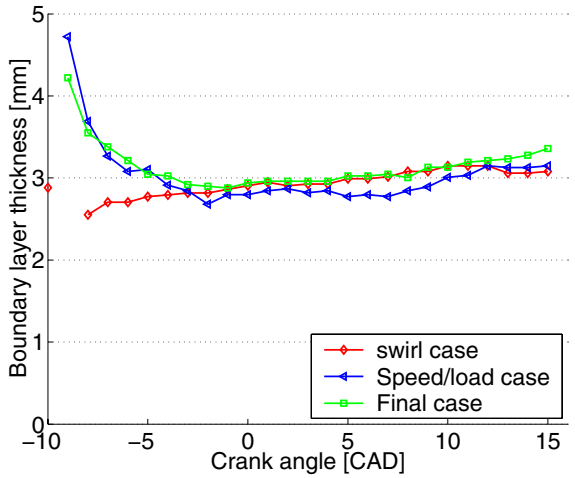

Figure 9. Boundary layer thickness for the three base cases.

SWIRL SWEEP

The swirl sweep consists of five measurements with increasingly blocked swirl valve, giving a swirl number from 2 to 2.6. The fully open swirl valve is the default setting used in all the other sweeps. So the “0% (open)” measurement is the reference case and one of the base cases discussed earlier. The intensity plots for this sweep can be seen in Figure 10 and the corresponding boundary layer thickness in Figure 11.

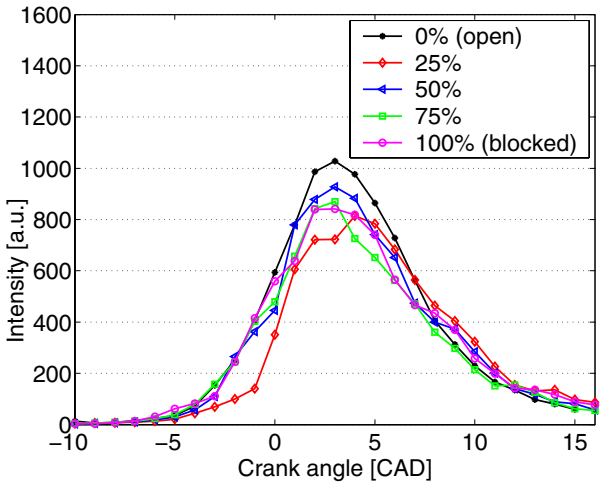

Figure 10. Maximum intensity for swirl sweep.

The intensity plots show no significant differences. The peak intensities seem to be only slightly lower with increasingly blocked swirl valve and it is unclear if the blocking is the reason. Furthermore, the case with 25% blocked intake appears to have slightly later timing.

The change in swirl and thereby turbulence caused by blocking one of the inlet ports appears to have no direct influence on HCCI combustion. Besides the just described low intensity differences, this statement is also approved by the minor changes in inlet temperature that is needed to keep constant combustion phasing. Furthermore, the burn duration displayed in Figure 8 is nearly constant for all measurements of the swirl sweep. A reason for this behaviour lies in the nature of HCCI combustion. It is generally accepted among researchers that the HCCI combustion process is controlled by chemical kinetics. This means that turbulent mixing does not affect the chemical reactions and heat release process during the main combustion because the local chemistry is an order of magnitude faster than turbulence effects. However, this explanation is only valid if no mass stratification exists, as this has been shown to increase the role of turbulence on combustion [12]. As PFI was used for the swirl sweep, no mass stratification is expected. The influence of mass stratification is investigated later in the DI sweep.

Regarding the boundary layer thickness for the swirl sweep in Figure 11, some obvious differences can be observed. The reference case with open swirl valve has a nearly constant thickness of about 3 mm. But with increasingly blocked valve a growing shifting of the thickness during combustion is visible leading to a thinner boundary layer in the first part and a thicker one in the last part of combustion. The intersection point where all cases have nearly the same boundary layer thickness is around 5 CAD ATDC.

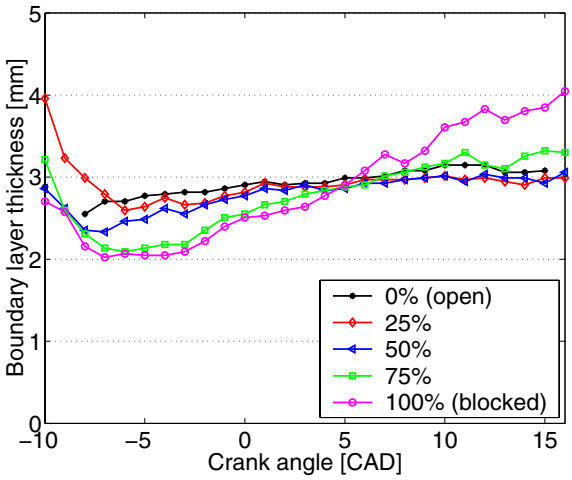

Figure 11. Boundary layer thickness for swirl sweep.

A recent paper by Aceves et al. [13] has indicated that geometry generated turbulence generates a thicker boundary layer and hence more thermal stratification resulting in a longer burn duration. The results of the measurements conducted in this swirl sweep do not allow the same conclusion for turbulence generated by blocking one inlet port. The increase in turbulence only leads to a thicker boundary layer towards the end of combustion. From -5 to +5 CAD ATDC the effect is just the other way around, meaning the boundary layer is thinner with more turbulence

The thinner boundary layer at increasing swirl seems to be a direct result of the increase in flow velocity, as all other parameters like burn duration and inlet temperature are nearly constant.

DIRECT INJECTION SWEEP

The direct injection sweep shows little difference in boundary layer thickness between the different cases as can be seen in Figure 12. For early injection timing from 180 to 90 CAD BTDC, nearly no changes in the boundary layer thickness are found. But for later injection the boundary layer seems to become thinner. The burn duration for the DI sweep in Figure 8 shows the same trend. For early injection it is nearly constant, but for later injection at 50 and 30 CAD BTDC the burn duration is much shorter. This similarity in behaviour brings out the assumption that there is a relationship between the boundary layer thickness and the burn duration.

Figure 13 gives an indication of the homogeneity for the different cases. The figure shows averaged images from both the lower camera through the piston extension and from the camera taking the horizontal images for boundary layer calculations. It can be seen that later injection leads to a less homogeneous combustion which also affects the horizontal intensity distribution of the side view image. While the side view of the 180 CAD case looks like all other sweeps with PFI, the cases with later injection timing show most of the combustion intensity in the right side of the side view image. To avoid unknown influences on the boundary layer calculation, the range for horizontal averaging for this sweep was reduced and set to the right half of the image where higher intensity levels are measured. The boundary layer thickness of the quite homogenous 180 CAD case that has been calculated in this way has the same level as other PFI cases. This indicates that this necessary adjustment in the calculation routine does not affect the comparability. However, it must be kept in mind that there may be some local differences in boundary layer thickness for the more inhomogeneous cases.

The intensities that are displayed in Figure 14 are analogous to the boundary layer calculation based on the adjustments described above. They show no significant differences. Only the 90 CAD case has generally lower intensity levels but without explainable reason.

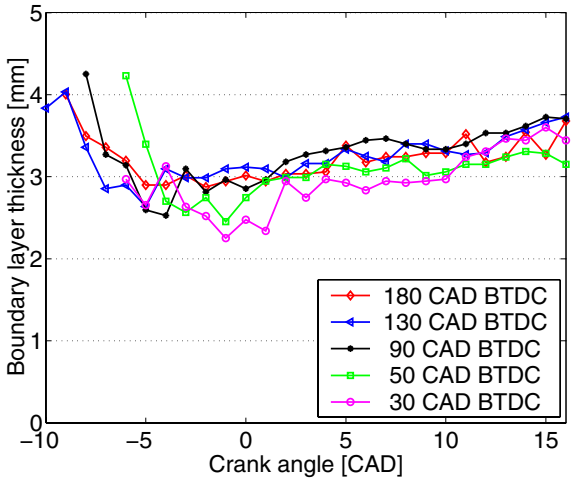

Figure 12. Boundary layer thickness for DI sweep.

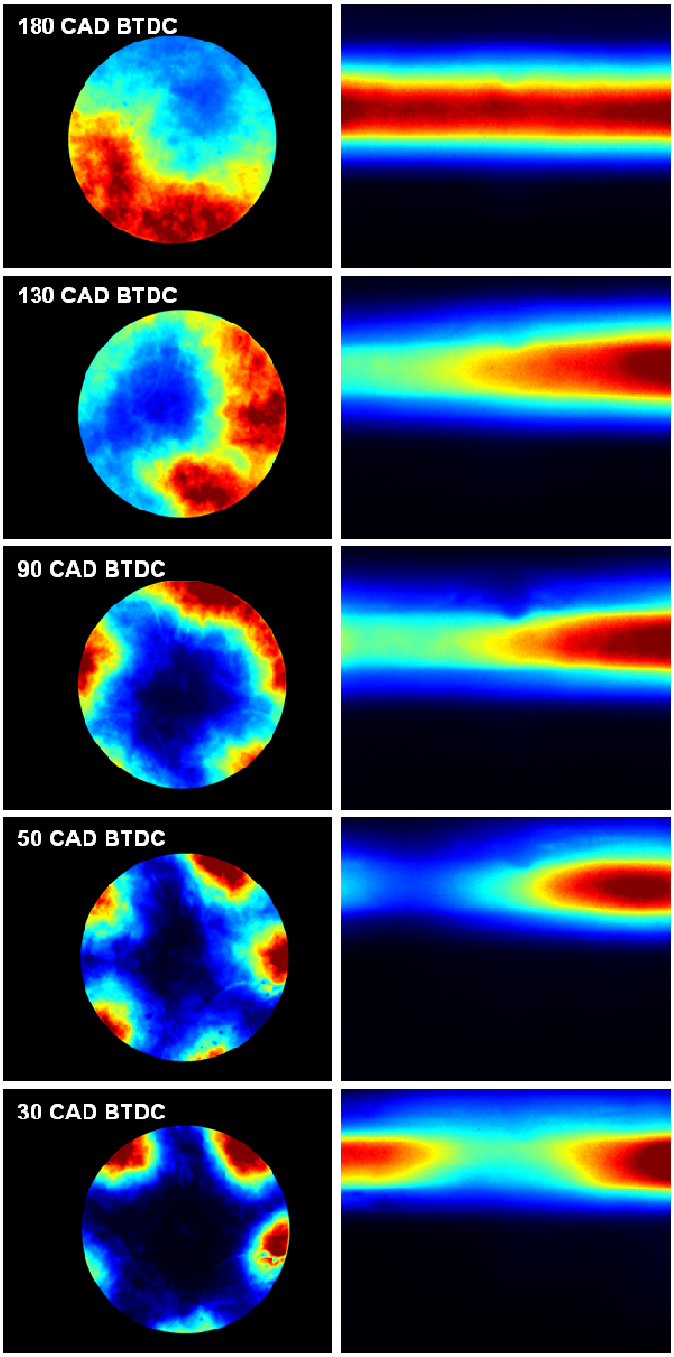

Figure 13. Comparison for DI with different injection timing, all taken at the point of CA50. Left images view from below, Right images side view used for boundary layer calculations.

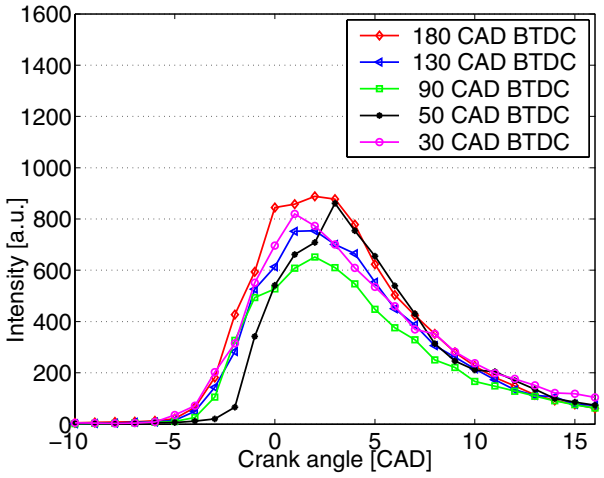

Figure 14. Maximum intensity for DI sweep.

LOAD SWEEP

For the load sweep, the reference case is included as the load at 2 bar IMEP. The combustion phasing was kept constant by controlling the inlet air temperature. Running higher loads was not possible because of limitations given by the optical access and inlet air temperature.

The calculated boundary layer thickness displayed in Figure 15 shows only minor differences. At lower loads, from 1.0 to 2.0 bar, the boundary layer thickness has nearly the same behaviour, which is slightly increasing with proceeding combustion. The apparently thicker boundary layer for the 1.0 bar case before TDC is probably not realistic as the intensity level and thus the SNR begins to rise later for this case. The high load case (3.0 bar IMEP) shows a different behaviour with a thinner boundary layer during the first half of combustion followed by a strong increase after 5 CAD ATDC. To exclude the possibility of a measurement error, this case was repeated, but the results only got verified by the second measurement.

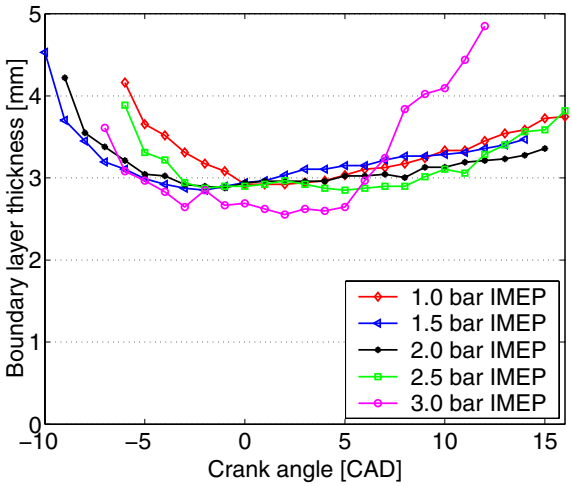

Figure 15. Boundary layer thickness for load sweep.

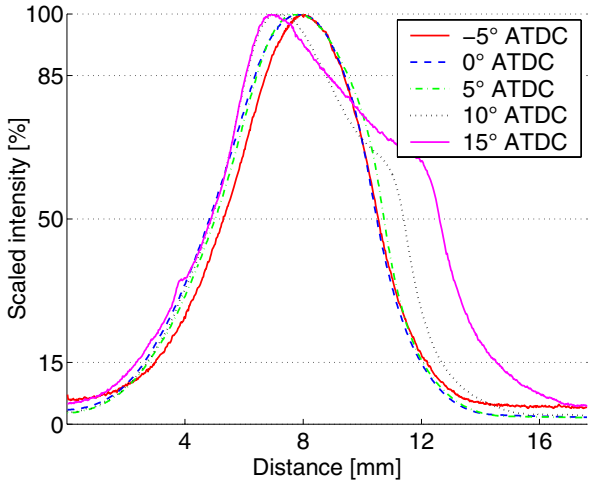

Figure 16. Scaled intensity for 3 bar case from load sweep at different CAD:s.

The phenomena can be explained by looking at Figure 16 displaying scaled intensities for different CAD:s for the 3 bar load case. On the intensity axis the 15% and 85% borders of the boundary layer definition are marked. The cylinder head is located at approximately 3 mm and the piston at approximately 12 mm moving even further for later crank angles. The maximum intensity for later CAD:s lies closer to the cylinder head and not in the middle of the combustion chamber. From the maximum towards the piston, the intensity first drops slowly to about 70% of the maximum before the same steep decrease as usual starts. During the first slow decrease, the intensity falls already below the 85% border and the area is per definition considered as part of the boundary layer. But as a steep temperature and thus intensity gradient is an essential characteristic for the boundary layer, the used boundary layer definition may not be accurate in this part of the sweep. Furthermore Figure 16 shows that the whole boundary layer moves closer to the cylinder head during combustion; if comparing at -5 and 15 CAD (solid lines) it is most obvious. This is probably due to the increased temperature during combustion.

The thinner boundary layer in the first part of combustion of the 3.0 bar case in combination with the lower burn duration shown in Figure 8 corresponds well to the assumption which has been established for the DI sweep. A shorter burn duration and thus faster combustion seems to lead again to a thinner boundary layer. In the other direction the relationship is not so definite. Although the burn duration is slightly longer for lower load, no significant difference can be seen in the boundary layer thickness. Perhaps the effect is neutralized in some way by the high inlet air temperature that is required to keep constant combustion phasing.

The faster burn rate and shorter duration for higher loads is also supported by the maximum intensity plots for the side view shown in Figure 17. It is clearly noticeable that higher load leads to higher intensity during the main combustion and to a steeper increase after ignition.

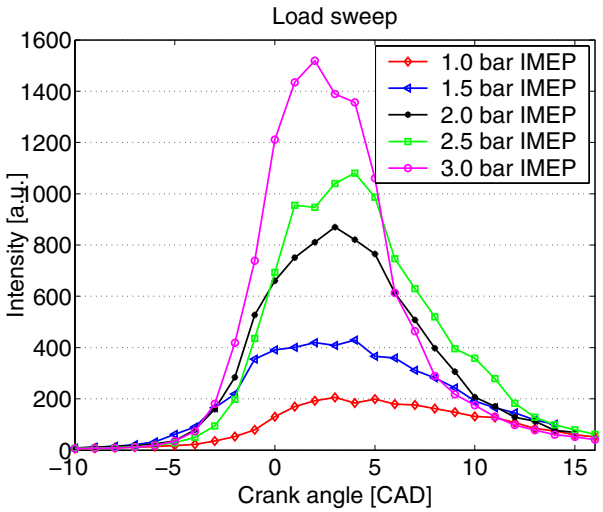

Figure 17. Maximum intensity for load sweep.

SPEED SWEEP

The speed sweep is run from 700 rpm up to 1500 rpm. The point at 1200 rpm is the speed/load reference case. In Figure 18 a slight decrease in boundary layer thickness can be seen for increasing speed, from 700 to 1500 rpm. The case at 1500 rpm has the smallest boundary layer; this can also be supported by the shorter burn duration shown in Figure 8. As the increase of engine speed comes along with strong increase of turbulence and flow velocity, this is probably the reason for the thinner boundary layer. From the start of the main combustion to the end all four cases show an increase in boundary layer thickness of about 0.5 mm each. The boundary layer for the case at 1500 rpm shows some inconsistency at the end of combustion, this is investigated and the reason shown in Figure 19 is the same as for the high load case. The threshold for the boundary layer calculations is above a plateau in the intensity towards the piston. For this case as well as for that shown in Figure 16 the upper boundary layer seems to move closer to the cylinder head during combustion.

The seemingly different behaviour of the 1500 rpm case before the main combustion allows no further conclusion. As explained before the results of the boundary layer calculation before ignition are not accurate because of a too low signal level. The 1500 rpm has the same bad SNR in this part of the measurement range, so that the seemingly better results here are probably just a matter of coincidence.

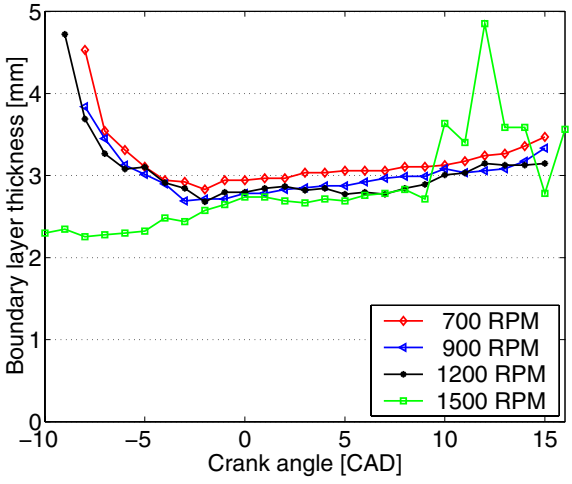

Figure 18. Boundary layer thickness for speed sweep.

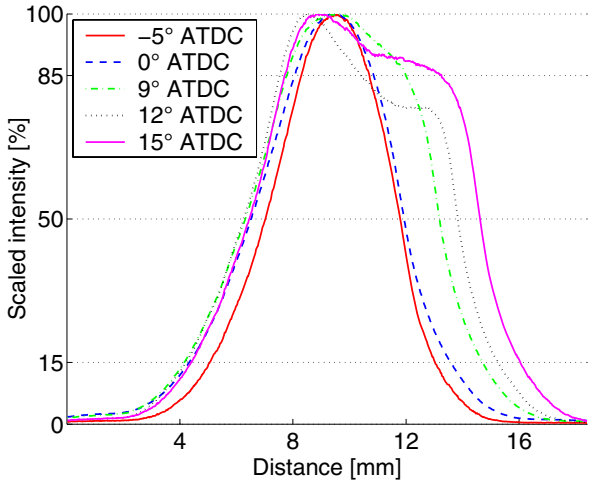

Figure 19. Scaled intensity for 1500rpm case from speed sweep at different CAD:s.

When looking at the maximum intensities in Figure 20 it shows that the combustion is slower at low speed giving less intensity but slightly longer duration. It should however be remembered that the intensifier gating time was kept constant in time, this has been compensated for afterwards by multiplying the intensities with the base case speed divided by the different speeds.

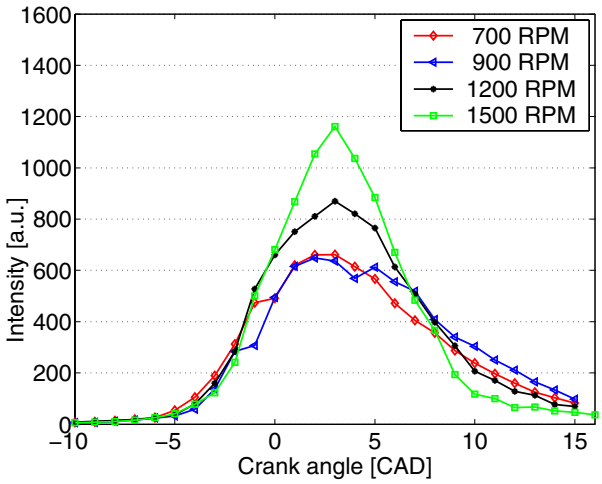

Figure 20. Maximum intensity for speed sweep with corrected intensities due to the difference in speed.

DISCUSSION

For all the cases studied, the boundary layer thickness is in the same order of magnitude. For the DI sweep a late injection, for the load sweep a high load and for the speed sweep a high speed all show shorter burn duration and a corresponding thinner boundary layer. A strong correlation between boundary layer thickness and the burn duration can be concluded. An explanation for this effect could be that shorter burn duration leads to a higher peak heat release and thus higher temporary temperatures which move the boundary layer closer to the wall, making it thinner. The boundary layer as such is shown to move closer to the wall during combustion. For the swirl case no change in combustion duration occurs; still the boundary layer behaviour changes. It does not however change in the same way as the other cases; instead it tilts more with a thinner boundary layer for the early combustion and then it gets thicker towards the end.

The average intensity is shown to have a strong linear correlation to the rate of heat release. Also the averaged maximum intensity seems to scale well with the rate of heat release according to Figure 3. The latter results also show this with increased maximum intensity for increased load, changes in burn durations in the same direction corresponding to those calculated from the pressure trace.

For all four sweeps it can be seen that the boundary layer gets slightly thicker at the end of combustion. Combustion occurs closer and closer to the wall as the in-cylinder temperature and the wall temperature increase during the combustion process, but still the heat release rate close to the piston doesn't increase to that of the core in the combustion chamber. Thereby the boundary layer gets thicker during the combustion.

In another publication [9] it has been seen that in the late combustion the intensity is higher close to the piston and to the cylinder head while the intensity is lower in the middle. In this study some similarity to this is shown for the highest load case (Figure 16) and for the highest speed case (Figure 19) where a plateau in the intensity can be seen at the late part of combustion. A reason for only seeing the phenomena for these cases can be that since it is an optical engine it is run with an although constant yet low cooling water temperature, so combustion is perhaps not as completed as in a hotter steel engine. This is supported by fairly high emissions of HC and CO.

CONCLUSIONS

A number of conclusions can be drawn from this experimental study:

- Chemiluminescence can be used as a tool for detecting combustion boundary layer behaviour in HCCI combustion.
- The averaged chemiluminescence intensity measured through the quartz liner and the averaged maximum intensity measured through the quartz liner both scale linearly against rate of heat release with high accuracy.
- Increasing swirl or speed (turbulence) leads to a thinner boundary layer.
- A thinner boundary layer correlates to faster burn duration.
- The boundary layer thickness is in the same order of magnitude for all cases and differs from 2 to 4 mm by the definition used.
- The boundary layer gets thicker towards the end of combustion.
- Changes in engine load and to some extent burn duration can be seen from the averaged maximum intensity.
- The entire boundary layer seems to move closer to the walls during the combustion.
- For more in-homogeneous cases, the location of the boundary layer measurements can affect the measured boundary layer thickness.

ACKNOWLEDGMENTS

The authors would especially like to thank the technicians at the division for making the engine and the measuring systems work and keep running.

REFERENCES

1. S. Onishi, S. Hong Jo, K. Shoda, P Do Jo, S Kato: ”Active Thermo-Atmosphere Combustion (ATAC) – A New Combustion Process for Internal Combustion Engines”, SAE Paper 790501
2. P. Najt, D. E. Foster: ”Compression-Ignited Homogeneous Charge Combustion”, SAE Paper 830264
3. M. Christensen, P. Einewall, B. Johansson: ”Homogeneous Charge Compression Ignition (HCCI) Using Isooctane, Ethanol and Natural Gas – A Comparison to Spark Ignition Operation”, SAE Paper 972874
4. J. Hyvönen, G. Haraldsson, B. Johansson: ”Balancing cylinder to cylinder variations in a Multi-Cylinder VCR_HCCI engine”, SAE Paper 2004-01-1897
5. H. Persson, R. Pfeiffer, A. Hultqvist, B. Johansson, H. Ström; “Cylinder-to-Cylinder and Cycle-to-Cycle Variations at HCCI Operation with Trapped Residuals”, SAE paper 2005-01-0130
6. J-O. Olsson, P. Tunestål, B. Johansson; “Closed-Loop Control of an HCCI Engine”, SAE Paper 2001-01-1031
7. G. Haraldsson, J. Hyvönen, P. Tunestål, B. Johansson; ”HCCI Closed-Loop Combustion Control Using Fast Thermal Management”, SAE Paper 2004-01-0943
8. S.B. Fiveland, D.N. Assanis; “Development of a Two-Zone HCCI Combustion Model Accounting for Boundary Layer Effects” SAE Paper 2001-01-1028
9. A. Hultqvist, M. Christensen, B. Johansson, A. Franke, M. Richter, M. Aldén; “A study of the Homogeneous Charge Compression Ignition Combustion Process by Chemiluminescence Imaging”, SAE Paper 1999-01-3680
10. A. Hultqvist, M. Christensen, M. Richter, J. Engström, A. Franke, B. Johansson; “Near-Wall Combustion in a Homogeneous Charge Compression Ignition (HCCI) Engine” International Symposium on Internal Combustion Diagnostics, pp 83-90, Baden-Baden, 2000
11. M. Christensen, B. Johansson, A. Hultqvist; “The Effect of Combustion Chamber Geometry on HCCI Operation” SAE Paper 2002-01-0425
12. Y.Z. Zhang, E.H. Kung, D.C. Harworth; “A PDF Method for Multidimensional Modeling of HCCI Engine Combustion: Effects of Turbulence/Chemistry Interactions on Ignition Timing and Emissions” Proceedings of the International Multidimensional Engine Modeling User’s Group Meeting, Detroit, 2004
13. S.M. Aceves, D.L. Flowers, J. Martinez-Frias, F. Espinosa-Losa, M. Christensen, B. Johansson, R.P. Hessel; “Analysis of the Effect of Geometry Generated Turbulence on HCCI Combustion by Multi-Zone Modeling”, SAE 2005-01-2134

Coresponding author:
Håkan Persson

Address
Lund Institute of Technology
Dept. of Heat and Power Engineering
Div. of Combustion Engines
P.O. Box 118
221 00 Lund
Sweden

E-mail
hakan.persson@vok.lth.se

ACRONYMS

ATDC	After Top Dead Center
BTDC	Before Top Dead Center
CAD	Crank Angle Degree
CI	Compression Ignition
CO	Carbon monoxide
DI	Direct Injection
HC	Hydrocarbons
HCCI	Homogeneous Charge Compression Ignition
IMEP	Indicated Mean Effective Pressure
IMEPnet	Entire cycle, including pump loop
LTR	Low Temperature Reaction
HTR	High temperature Reaction
PFI	Port Fuel Injection
SI	Spark Ignition
SNR	Signal to Noise Ratio

APPENDIX

A linear regression is used to point out the correlation between the rate of heat release and intensity. To quantify this relationship the coefficient of determination R^2 is calculated by the following expression:

$$R^2 = \frac{\left[\sum_{i=1}^{n}(x_i - \bar{x})\cdot(y_i - \bar{y})\right]^2}{\sum_{i=1}^{n}(x_i - \bar{x})^2 \cdot \sum_{i=1}^{n}(y_i - \bar{y})^2}$$

where n is the number of pairs of data, x_i and y_i the actual value for the i-th CAD, $\bar{x}$ and $\bar{y}$ the mean values. The coefficient of determination is the square of the correlation coefficient and denotes the strength of the linear association between x and y.